Optical and morphological study of disorder in opals

E. Palacios-Lidón, B. H. Juárez, E. Castillo-Martínez, and C. López[a)]
Instituto de Ciencia de Materiales de Madrid, (CSIC) Sor Juana Inés de la Cruz 3, 28049-Madrid, Spain

(Received 7 October 2004; accepted 3 December 2004; published online 1 March 2005)

An optical and morphological study has been carried out to understand the role of intrinsic defects in the optical properties of opal-based photonic crystals. By doping poly(methylmethacrylate) (PMMA) thin-film opals with larger polystyrene (PS) spheres, structural disorder has being generated perturbing the PMMA matrix periodicity. It is shown that this disorder dramatically affects the optical response of the system worsening its photonic properties. It has been found that the effect of doping is highly dependent not only on the concentration but also on the relative size of the dopant with reference to the matrix. Through a detailed scanning electron microscopy inspection, the sort of structural defects involved, derived from the different particle size used, has been characterized. A direct relationship between the observed optical response with the different perturbations generated in the lattice has been found. In addition, from this study it can be concluded that it is possible to grow high quality alloyed photonic crystals, exhibiting intermediate photonic properties between pure PMMA and pure PS opals by simple sphere size matching and variation of the relative concentration of both components. © *2005 American Institute of Physics*.
[DOI: 10.1063/1.1851014]

I. INTRODUCTION

The achievement of light path routing has fostered the development of photonic crystals[1,2] (PCs) in the last decades. The optical response of a PC is determined by the periodic modulation of the refractive index that, in turn, is directly affected by the crystallographic quality of the actual structure. Thus, the presence of any sort of structural disorder makes the PC depart dramatically from the ideal behavior, reducing or even destroying its photonic properties.[3]

One of the cheapest route to three-dimensional (3D) PCs working in the near-infrared–visible range is represented by close-packed arrays of spherical colloids of micron-sized self-assembled in a fcc lattice, opal-based PCs.[4] Due to an unavoidable variation in the opal sphere size (polydispersity) and probable stacking faults, the presence of randomly distributed, uncontrolled defects in PC is an inherent feature associated with the crystal growth process from a colloidal state.[5] Much effort has been devoted to improving design, for example by infiltration with different materials,[6] to tune the optical response of a PC. However, there is lack of references listed in the literature concerning the effects of disorder in 3D PCs, mainly those performed in usual opals obtained by sedimentation.[7–9] This situation may be understood taking into account the difficulties to introduce different types of disorder in this sort of material in a controlled manner, and the subsequent quantification of their effects on the photonic behavior. Minimization of the amount of disorder present in the final product and knowledge of how it affects the photonic properties are important tasks to be tackled before technological applications are made in the future.

Numerous studies have been concerned with self-assembling of spheres of different sizes by sedimentation of a suspension of two populations to form binary crystals.[10–12] The aim was the achievement of stoichiometric ordered crystals, exhibiting structures similar to those found in well known atomic systems, such as NaCl, CsCl, or ZnS,[13] through variations in the concentrations and particle diameter ratios of the components. By mixing colloidal suspensions of two components with different particle diameters, it is also possible to introduce a certain sort of disorder in the final product. In a previous report,[14] it was shown that the photonic response deteriorates progressively as the degree of disorder rises by increasing concentrations of small polystyrene (PS) spheres embedded in a PS opaline matrix of larger spheres.

The aim of this article is to characterize from a structural point of view the disorder in PCs, and to analyze its effect on the optical response. Thin films of well-ordered poly(methylmethacrylate) (PMMA) have been perturbed by adding different amounts of larger PS spheres of different sizes as dopants during the assembly process. It has been found that the optical properties are highly dependent not only on the concentration but also on the relative dopant sphere size. Through a detailed inspection of samples in their respective scanning electron microscope (SEM) pictures, the sort of defects generated from the different particle sizes used has been characterized. A direct correlation of changes in optical response and the different perturbations generated in the lattice has been found. Sphere populations of different chemical nature have been used, first because when the dopant size is much larger than the host one, the density difference[15] between them (the PS is less dense than the PMMA) makes it possible to obtain a homogeneous suspension needed to enhance uniform crystal growth. Second and more important, when the spheres of the two components are of the same size, photonic alloys with no structural defects present, except those associated with intrinsic polydispersity of the col-

[a)]Electronic mail: cefe@icmm.csic.es

loids themselves, can be obtained. These compound systems present an optical behavior characterized by magnitudes that can be approximated by weighted averages of their individual components.

II. EXPERIMENTAL SECTION

Monodisperse PMMA (polydispersity $<3\%$) and PS ($<5\%$) spheres were independently synthesized by an emulsion polymerization method in the absence of surface active agents.[16,17] The reaction mixture was filtered through glass wool and exhaustively cleaned by several cycles of centrifugation and redispersion. The final product appears as a milky aqueous suspension of spheres whose particle concentration was estimated from the density of PS and PMMA using a dry-out method.

Thin artificial opals were prepared by vertical deposition methods on glass substrates.[18] Substrates and vials were previously cleaned with hydrochloric acid 36 vol % solution (Fluka) for 24 h and subsequently rinsed with double distilled water. Diluted aqueous suspensions of PMMA spheres (0.33 vol %) were prepared. In order to control the number of dopants in each case some amount of PMMA spheres were substituted for the same amount of PS spheres keeping the number of spheres constant in all cases. A homogeneous distribution of the PS spheres in the aqueous suspension of PMMA spheres was obtained by strong sonication. All the samples were grown in an oven at 47 °C for 16 h. By using this method, samples of about 1 cm^2 and up to 55 layers thick were obtained. It is important to prepare thick enough samples (at least 30 layers) in order to prevent the appearance of finite size effects that affect the position, line shape, and intensity of the Bragg peak,[19] which would make the analysis of the experimental data difficult.

The optical response of the PCs thus prepared has been studied by reflectance measurements using a commercial Fourier Transform infrared (Bruker IFS 66 with IRScope II). Zones up to 1 mm^2 were tested in order to assure homogeneous optical response with good average in defect distribution. Samples presenting strong variations in the reflectance intensity in different areas were discarded, considering that they were not representative for the present work. The morphological study of the samples has been done by SEM inspection. Although only a few samples are shown, all the samples where exhaustively examined, checking the surface and cleaved edges and confirming the homogeneous distribution of the dopants in the host (Fig. 1) and that no phase segregation occurred. Thus, the behaviors described here are representative of all the samples and not particular cases.

III. OPTICAL CHARACTERIZATION

It is well known that the presence of a defect in a PC, in analogy with the behavior observed for electron crystals, introduces localized states within the energy gap in a well-defined position.[20,21] If the defects are randomly distributed, the optical response is given by the average of all defect configurations, resulting in a decrease of the Bragg peak intensity.[22] One way of introducing structural disorder in an artificial opal is by adding a controlled amount of dopant

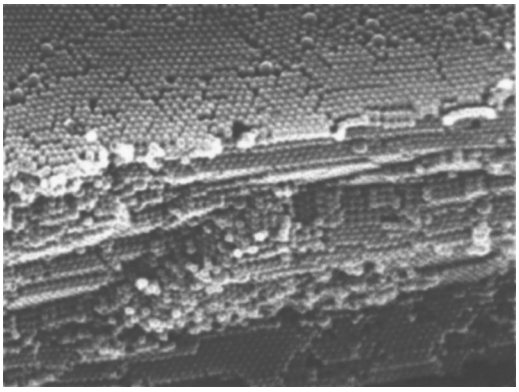

FIG. 1. Cleaved edge of a sample consisting of a thin-film opal of 270-nm PMMA spheres doped with 0.1% of 700-nm PS colloids. The large PS spheres can be clearly distinguished throughout the sample.

spheres of sizes different from those of the host, as shown in Fig. 1. High quality "defect-free" samples are needed to be used as reference, to study the effects derived from the dopants addition. By using the vertical self-assembly convective method, good quality monocrystalline samples are obtained. These samples show a high reflection Bragg peak even if an inherent disorder due to the spheres polydispersity and to the unavoidable cracks arising during the drying process,[19] is present. These unavoidable defects must be considered an inherent constant to the method of preparation, and are supposed to equally affect defect-free and doped samples.

The reflectance spectra of PMMA thin-film opals of 270-nm spheres doped with different concentrations (from 0% to 1%) of 700-nm PS spheres are shown in Fig. 2. As expected, the Bragg peak intensity decreases as the PS number of spheres increases in agreement with previous results reported by Gates *et al.*[14] This feature proves that the structural disorder in the PC increases with the number of dopants in the matrix. It is noteworthy that the line shape of the Bragg peak changes abruptly when a certain value of doping is reached. This effect can be understood in terms of the band structure evolution and will be the subject of future work. The oscillations appearing at both sides of the Bragg peak which are associated with the finite thickness of opal film are an indication of homogeneity and thus, of order. These oscillations only appear in samples with no impurities or very low doping.

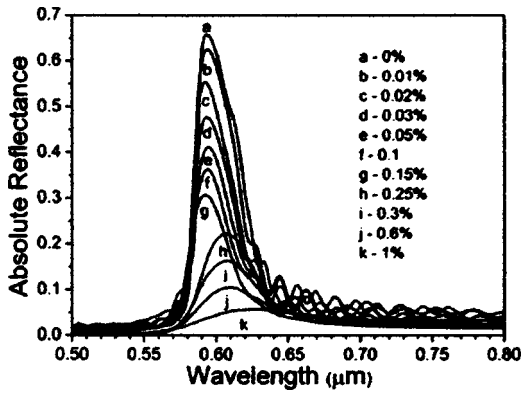

FIG. 2. Reflectance spectra of a 270 nm thin-film PMMA opal doped with concentrations ranging from 0% to 1% of 700-nm PS spheres.

TABLE I. Diameter of the PS dopants (d_{PS}), ratio the sizes of the two spheres ($\alpha = d_{PMMA}/d_{PS}$), and concentrations (c_{PS}) ranges used on each of the series. The PMMA sphere size is 270 nm for the three series.

	d_{PS} (mm)	α	c_{PS} (%)
Series A	700	2.59	0–1
Series B	450	1.67	0–3
Series C	350	1.3	0–30

To study the optical reflectance dependence on the host/dopant sphere diameter ratio, several samples were prepared by adding PS spheres of different sizes and keeping the host sphere size constant. The PS sphere diameter, the dopant/host diameter ratio (α), and the dopant concentration used for each sample are listed in Table I.

The respective reflectance measurements [Figs. 3(a)–3(c)] show that, although the Bragg peak intensity decreases as the dopant concentration increases, the concentration needed to destroy the photonic behavior of the crystal is highly dependent on diameter ratio, being lower as the relative size of the dopant increases.

In Fig. 4, the detrimental effect on the intensity of the peak when different sizes of impurities are added to the lattice in the same concentration (0.1%) is shown. When the host and guest spheres are close in size ($\alpha = 1.3$), the reflectance intensity of the Bragg peak becomes almost identical to that of the defect-free sample. Opposite behavior is found, however, in the case of very different sizes for guest and host spheres so that, for the same dopant concentration, the Bragg peak almost disappears.

IV. MORPHOLOGICAL CHARACTERIZATION

In order to characterize the defects introduced in the host by dopant addition, a detailed SEM study has been carried out. Three samples with low, medium, and high dopant content have been selected from each of the series A B, and C. In order to compare samples with similar intensities of the corresponding Bragg peaks, it was necessary to use samples of series C with concentrations of 0.1%, 1%, and 10%. This means one order of magnitude higher than those of samples corresponding to series A (0.01%, 0.1%, and 1%) and to series B (0.02%, 0.1%, and 1%). For lightly doped samples, the disorder generated by each PS particle is isolated and can be studied individually. However, as the number of impurity particles increases, the defects created by different particles finally interfere.

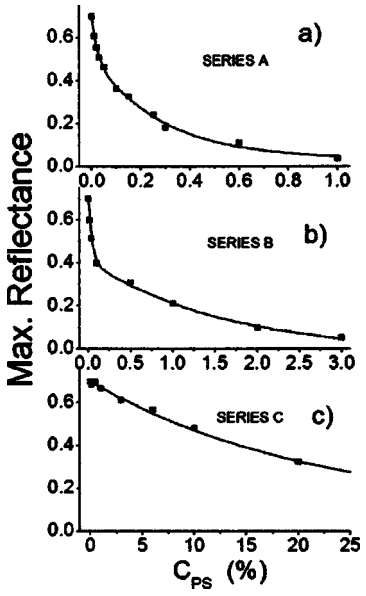

FIG. 3. Maximum reflectance intensity for the three series as a function of dopant concentration: (a) $\alpha = 2.59$, (b) $\alpha = 1.67$, and (c) $\alpha = 1.3$. A decreasing tendency is clearly seen in the three situations, although the doping concentration needed to destroy the photonic behavior markedly differs. Solid lines are fit with Eq. (3) and parameters in Table II.

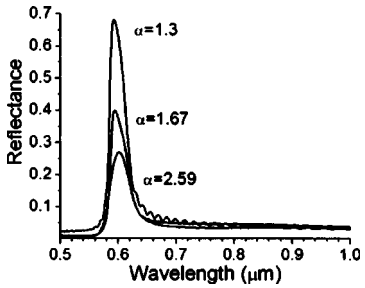

FIG. 4. Reflectance response for three opals doped with the same amount of guest spheres (0.1%) but different dopant-to-host size ratio.

The types of defects formed by the presence of dopant spheres in artificial opals are similar to those found in atomic crystals[23] and they can be classified as point, line (dislocations), or planar (stacking faults, grain boundaries, etc) defects. By using the vertical convective method, monocrystalline samples are grown with [111] the zone axis normal to the surface. Neither grain boundaries nor mosaic spread are found.[19] The only types of defects observed in these arrangements are point defects, dislocations, stacking faults, and cracks.

Since perfect PCs are periodic in nature, structural defects, which result in a breaking of periodicity, can be more precisely analyzed in reciprocal space. In order to do so, SEM images have been processed by a fast Fourier transform (FFT) algorithm.[24] The FFT images obtained show bright spots for single crystals or rings for polycrystalline samples, and contain information of the lattice periodicity. Crystal defects appear as randomly distributed points (diffuse) or grouped along crystallographic directions (dislocations and stacking faults). For amorphous materials, the FFT images consist of ill-defined diffuse halos. The presence of structural defects always affects the power spectrum by decreasing the spot intensities and increasing the diffuse background. In this study, the absolute intensity is not considered as it is determined by the contrast of the SEM photograph. However, it is possible to compare relative intensities by normalizing the images to the zero order spot that is always the most intense one. Disorder can be qualitatively estimated through the respective spot intensity ratio.

Figure 5 shows the SEM images along with their FFT treatment and line profiles for three representative concentrations of series A samples. In this particular case and due to the relatively large size of the doping colloids, their inclusion in the matrix produces strong perturbations. The overall ap-

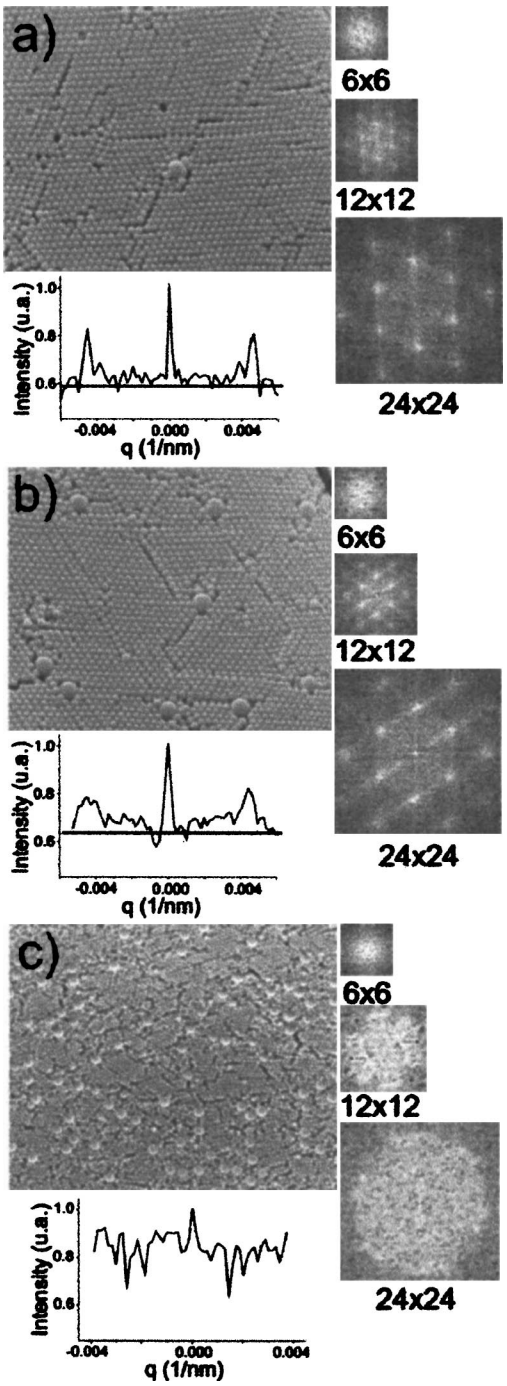

FIG. 5. SEM photographs, FFT images, and intensity profiles of thin-film opals of 270-nm spheres doped with different concentrations of 700-nm colloids: (a) 0.01%, (b) 0.1%, and (c) 1%. The FFT images have been obtained from increasing areas (6×6, 12×12, and 24×24 spheres) centered in a PS dopant colloid.

pearance (real space) and the respective average FFT images (reciprocal space) obtained from progressively increasing areas containing 6×6, 12×12, and 24×24 PMMA spheres around each of the PS spheres are shown. In the sample with low dopant concentration [Fig. 5(a)], FFT images show that around a big PS particle of dopant a short-range disruption of the periodicity (extended to about three unit cells) is created. In long-range images (12×12 and 24×24), however, the threefold symmetry characteristic of zone axis [111] in an fcc lattice is clearly evidenced. Additional disorder associated

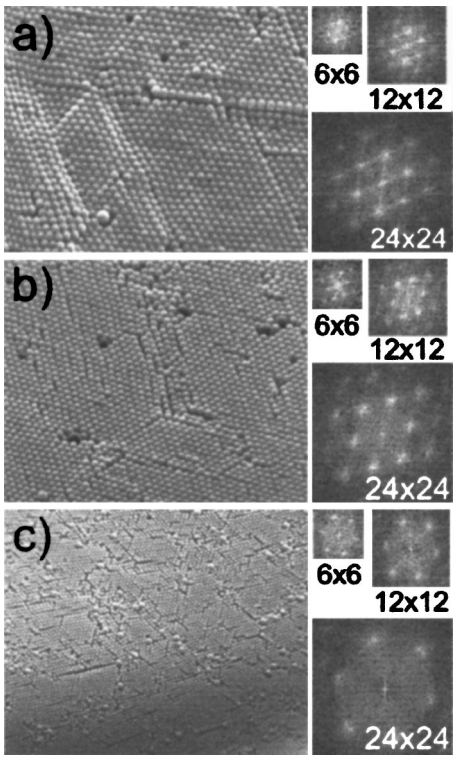

FIG. 6. SEM photographs (left panel), FTT images (right panel) of thin-film of 270-nm spheres opals doped with different concentrations of 450-nm colloids: (a) 0.02%, (b) 0.1%, and (c) 1%.

with the presence of dislocations and stacking faults is also present, as deduced from the straight lines connecting Bragg spots along crystallographic directions. In the intermediate concentration sample [Fig. 5(b)], the description of the defects generated by PS spheres is qualitatively similar to those in the low concentration sample because the PS spheres are kept apart and defects do not yet interfere. On the contrary, as the dopant concentration increases [Fig. 5(c)], individual dopant effects overlap and the long-range periodicity is perturbed.

Additional evidence is gained through intensity line profiles taken along symmetry directions. For the low doping concentration sample, sharp peaks corresponding to bright spots are superimposed over a weak diffuse background due to the localized defects. As the dopant PS concentration increases, although the periodicity is still evidenced, the peaks become broader and less intense, while the background signal increases. At 1% of PS impurity concentration, the diffuse background becomes so high that the peaks corresponding to long-range periodicities are no longer seen, as expected for an amorphous material.

For PS spheres of intermediate size (Fig. 6), the partial replacement of host spheres by PS dopant becomes less aggressive and the local disorder around the impurity is smaller. This can be appreciated in the FTT images even from the smallest area (6×6 spheres) where the periodicity is maintained. Again, the inclusion of PS dopant spheres of different sizes produces dislocations along the symmetry planes. As the doping concentration increases, the number of generated dislocations rises, and crossings lock up their propagation. The overall effect is a slight misorientation of

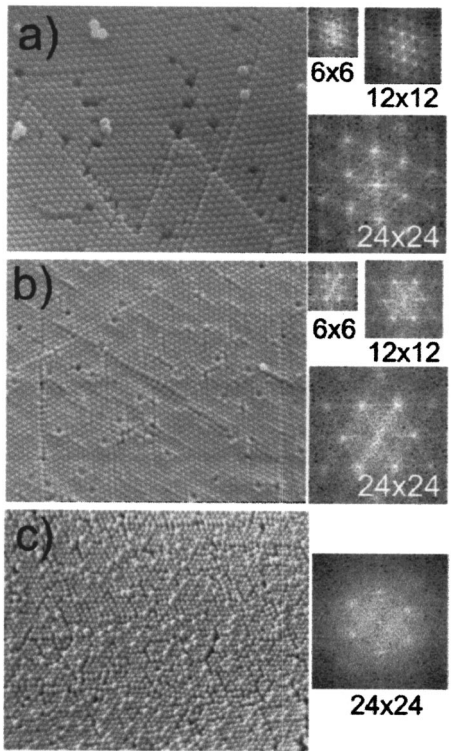

FIG. 7. SEM photographs (left panel), FTT images (right panel) of thin-film opals of 270-nm spheres doped with different concentrations of 350-nm colloids, (a) 0.1%, (b) 1%, and (c) 10%. In the most heavily doped sample (10%), the concentration of PS colloids is so high that the sample can not be considered a doped crystal but a binary one.

the domains in the surface plane. This is even more marked in the sample with highest doping concentration in which, although the periodicity is nearly broken, the residual Bragg spots present clear rocking shapes [Fig. 6(c)].

As the host/dopant ratio tends to unity (Fig. 7), dopants are easily integrated in the matrix with minor perturbations. In fact, no disrupted disorder around PS spheres is observed, and the only defects found are eventual point vacancies and dislocations extending far apart through long distances. For the sample with the highest PS dopant concentration (10%), the number of PS spheres is so high that obtaining an FFT image, even from the smallest area with less than two dopant particles, becomes impossible. Although the crystal should be considered an alloy rather than a doped crystal, there is still a residual long-range periodicity. In the three series, it has been found that as the disorder rises, the crystal becomes less compact and the lattice parameter increases.

V. PHOTONIC ALLOYS

From the results just presented, it must be concluded that if two populations of spheres, having the same size, are mixed, forming a PC, no structural defects would appear. In previous reports,[25] it was found that when the dopant-to-host diameter ratio approaches 1, no ordered phases are obtained. The spheres of two different materials are randomly distributed throughout the lattice forming a disordered alloy. In order to study the optical properties of these compound crystals, samples with PMMA and PS spheres of 242 and 252 nm, respectively, were prepared.[26] The relative concentrations of PS spheres in the PMMA matrix were 0%, 25%, 50%, 75%, and 100%, and 0% and 100% samples corresponding to the pure PMMA and PS opals, respectively. Under the assumption that no structural defects are produced, no strong variations in the reflectance intensity would be expected. This is confirmed by optical spectroscopy as shown in Fig. 8, where different reflectance spectra for several PS concentrations are shown. The peak intensity is similar for all of them, except perhaps for the pure PMMA sample. This feature can be caused by the higher polydispersity of PS beads in comparison to the PMMA ones, which implies higher inherent morphological disorder. However, these differences are small compared with the case in which spheres are of different sizes, as shown in Sec. IV.

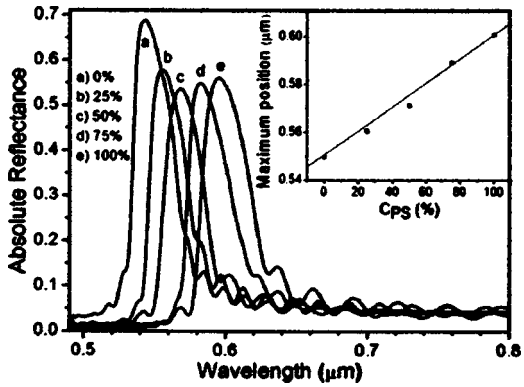

FIG. 8. Reflectance measurements of binary PMMA/PS crystals for increasing PS sphere concentrations. Inset: maximum reflectance intensity peak position. The solid line is the theoretical prediction following the Bragg law with average diameter and refractive index.

Due to the different refractive indexes of the two polymer spheres, the refractive index of the opal is a weighted average of the two. The position of the first pseudogap in the (111) direction can be estimated applying the Bragg law at normal incidence,[27] as

$$\lambda = 2d_{111}\langle n_{\mathrm{eff}}\rangle = 2(2/3)^{1/2} d_{\mathrm{eff}} n_{\mathrm{eff}}, \tag{1}$$

where n_{eff} can be approximately calculated as

$$\langle n_{\mathrm{eff}}\rangle = \langle \varepsilon_{\mathrm{eff}}\rangle^{1/2} = \{0.26 + 0.74[(1-x)\varepsilon_{\mathrm{PMMA}} + x\varepsilon_{\mathrm{PS}}]\}^{1/2}, \tag{2}$$

and $d_{\mathrm{eff}} = [252x + (1-x)242]$, x being the concentration of PS spheres. The refractive index of the PMMA and PS spheres has being taken as $\varepsilon_{\mathrm{PMMA}} = 1.5$ and $\varepsilon_{\mathrm{PS}} = 1.6$, respectively. When Eq. (2) is plotted along with the experimental Bragg wavelengths (Fig. 8 inset), a good agreement between the theoretical and experimental results is found. Notice that no fitting parameters are used.

VI. DISCUSSION

When a sphere of radius r_{m} in a matrix crystal is replaced by a larger dopant sphere of radius r_{d} a perturbation related with the strain parameter $\delta r / r_{\mathrm{m}}$, where $\delta r = r_{\mathrm{d}} - r_{\mathrm{m}}$, is created.[28] The large strains generated in the matrix, mostly concentrated around defects, lead to stress relaxation through plastic deformations. Since this sort of defects highly influences the mechanical and electrical properties of many ma-

terials it has been extensively studied (especially in metallic systems) for years. Defects associated with spherical intrusions[29] are highly dependent on the elastic constants of the host material (Young's modulus), and matrix relaxation takes place mainly in an area localized around the impurity. This region is often called the deformation zone and its size is proportional to the dopant-to-host volume ratio. It is characterized by the presence of small randomly oriented subgrains separated by thin walls of largely disordered material. Additionally, residual strains also relax through dislocations emerging from the inclusion particle and forming a plastic slip that is usually known as an Orowan loop.[30]

In the doped artificial opal samples, these two kinds of defects are clearly evidenced in SEM micrographs directly, as well as in reciprocal space through power spectrum images obtained by FFT. Short-range disorder, consisting of localized disruption of the matrix periodicity, is formed around the dopant particle, extending only along a few unit cells. Long-range disorder arising as well from the dopant colloid but extending along many unit cells is associated mainly with the presence of dislocations and stacking faults. These two types of defects may affect differently the intensity distribution of the reflected light in a reflectance spectrum.[31] Drawing attention to localized defects, the sample can be described as a periodic photonic matrix containing amorphous inclusions of size proportional to the volume ratio. At very low doping concentrations, the generated local defects are randomly distributed, acting as incoherent scattering centers whose presence reduces the Bragg peak reflection intensity dramatically. By increasing the dopant size (size of inclusion damage) or the dopant concentration (increase of the number of inclusions), the amount of amorphous material eventually becomes larger than that of the crystalline one and the sample loses periodicity completely. In this case, it no longer makes sense to talk about a PC. The presence of long-range perturbations associated with dislocations and stacking faults are not as destructive for the photonic behavior as those due to localized defects. This is because, although many lattice cells are slightly perturbed, the crystal periodicity is still preserved on average[7] and, consequently, the reflectance measurements are not so greatly affected. These considerations help to understand the optical response exhibited by the differently doped samples. When the dopant spheres are large compared with those of the host, the optical response is determined mainly by the presence of localized defects around dopant spheres. This effect is even observed in reflectance measurements of samples with a very low dopant concentration (0.01%). As the dopant concentration rises the respective deformation regions associated with the presence of dopant spheres quickly overlap producing amorphization of the overall system. If the dopant-to-host sphere size ratio tends to 1, the local disorder generated by each colloidal sphere becomes negligible and the overall photonic behavior of the sample is determined only by the presence of long-range disorder. These features explain the non-null Bragg peak intensity found in samples with the highest dopant content. These results are in agreement with those in Ref. 14, in which the size of dopant spheres were smaller than those of the host. In this case, disorder was associated mainly with the presence of dislocations and point defects that decreased the domain size. No short-range defects around each dopant sphere were evidenced showing that PCs admit the presence of high amounts of defects without destroying their photonic behavior.

TABLE II. Data of the exponential fitting. The parameters correspond to those in Eq. (3).

	A_1	t_1	A_2	t_2	Chi^2/degrees of freedom
Series A	0.19	46.0	0.48	3.5	2.0×10^{-4}
Series B	0.29	2.0	0.43	0.6	1.7×10^{-4}
Series C	0.0	0.0	0.62	0.046	2.2×10^{-24}

Looking for an analytical expression relating the Bragg peak intensity (R) decay with the amount of structural disorder, it is found that it can be empirically fitted by a linear combination of two exponential functions given by

$$R(\alpha, c_{\mathrm{dop}}) = A_1(\alpha)\exp[-c_{\mathrm{dop}}t_1(\alpha)] + A_2(\alpha)\exp[-c_{\mathrm{dop}}t_2(\alpha)], \quad (3)$$

where A_1, t_1, A_2, and t_2 are fitting parameters (Table II) dependent on the size ratio of the spheres. Fitting, as deduced from the chi-squared function, is fairly good and, consequently, finding of a physical meaning for the fitting parameters found would be desirable. The intensity decay of the Bragg peak seems to be the sum of two different contributions vanishing as the size ratio tends to 1. The authors suggest that these two different contributions may be due to the two different sources of disorder shown earlier. The first term might be associated with the presence of short-range disorder affecting dramatically the reflectance intensity of the Bragg peak when the size ratio is large. As the size ratio tends to unity, it sharply tends to zero, being negligible even in samples of the series C. The second term might be due to the presence of long-range disorder, which is always present if the dopant size is different from that of the host spheres. The amounts of dislocations and stacking faults also increase as the size ratio rises, as can be shown in the SEM images. However, a deeper understanding is needed to completely explain the optical response of a disordered PC, a work still in progress.

These results should be taken into account when artificial opal samples are prepared. If, as is usually found in silica spheres, polydispersity has a broad Gaussian distribution,[32] the optical response of the sample will be limited by long-range disorder. Polymer-based opals (PS, PMMA, or modifications of them) often present a much narrower Gaussian distribution than silica-based opals, although they usually present polydispersity associated with a second nucleation process.[16,17] Small amounts coming from this second nucleation cause worsening in the photonic properties of the crystal. Similar behavior is expected from the presence of impurities due to dust particles or organic residues from the sphere synthesis. This means that, although the growth method used is important, the quality of the final product might also be determined by the distribution of sphere sizes and cleaning process during the preparation.

VII. CONCLUSIONS

In this article, the effects of structure disorder in the photonic response of thin film opals have been studied by controlling the doping concentration and the dopant-to-host size ratio. It has been proved that both the concentration and size of dopants dramatically affect the photonic properties of the resulting PC. To explain the dependence of the reflectance Bragg peak intensity decay, a very simple two-contribution model is proposed. This hypothesis is supported with a morphological study showing that each dopant creates two well-differentiated types of disorder. The first one is the short-range disruptive disorder localized around the dopant spheres that strongly affects the photonic response, and the second one is a less aggressive long-range disorder consisting mainly of dislocations and stacking faults. The feasibility of growing photonic alloys that show optical properties that are weighted average of the individual components has been also shown.

ACKNOWLEDGMENTS

This work is partially financed by the Comunidad Autónoma de Madrid through a PhD grant (E. P.-L.) and 07T/0048/2003 project and the Spanish CICyT through MAT2003-01237 project.

[1]E. Yablonovitch, Phys. Rev. Lett. **58**, 2059 (1987).
[2]S. John, Phys. Rev. Lett. **58**, 2486 (1987).
[3]Z. Li and Z. Zhang, Phys. Rev. B **62**, 1516 (2000).
[4]R. Mayoral, J. Requena, J. S. Moya, C. López, A. Cintas, H. Míguez, F. Meseguer, A. Vázquez, M. Holgado, and A. Blanco, Adv. Mater. (Weinheim, Ger.) **9**, 257 (1997).
[5]V. N. Astratov, Phys. Lett. A **222**, 349 (1996).
[6]For a recent review in systems based on opals, see C. López, Adv. Mater. (Weinheim, Ger.) **15**, 1680 (2003), and references therein.
[7]Y. A. Vlasov, M. A. Kaliteevski, and V. V. Nikolaev, Phys. Rev. B **60**, 1555 (1999).
[8]Y. A. Vlasov, V. N. Astratov, A. V. Baryshev, A. A. Kaplyanskii, O. Z. Karimov, and M. F. Limonov, Phys. Rev. E **61**, 5784 (2000).
[9]V. N. Astratov, A. M. Adawi, S. Fricker, M. S. Skolnick, D. M. Whittaker, and P. N. Pusey, Phys. Rev. B **66**, 165215 (2002).
[10]P. Bartlett, R. H. Ottewill, and P. N. Pusey, Phys. Rev. Lett. **68**, 3801 (1992); P. Barlett and P. N. Pusey, Physica A **194**, 419 (1993).
[11]P. D. Kaplan, J. L. Rouke, and D. J. Pine, Phys. Rev. Lett. **72**, 582 (1994).
[12]A. B. Schofield, Phys. Rev. E **64**, 051403 (2001).
[13]X. Cottin and P. A. Monson, J. Chem. Phys. **102**, 3354 (1995).
[14]B. Gates and Y. Xia, Appl. Phys. Lett. **78**, 3178 (2001).
[15]The PS density is 1.05 g/cm^3 and the PMMA one is 1.19 g/cm^3.
[16]W. Goodwin, J. Hearn, C. C. Ho, and R. H. Ottewill, Colloid Polym. Sci. **252**, 464 (1974).
[17]M. Egen and R. Zentel, Chem. Mater. **14**, 2176 (2002).
[18]P. Jiang, J. F. Bertone, K. S. Hwang, and V. L. Colvin, Chem. Mater. **11**, 2132 (1999).
[19]J. F. Galisteo-López, E. Palacios-Lidón, E. Castillo-Martínez, and C. López, Phys. Rev. B **68**, 115109 (2003).
[20]E. Yablonovitch, T. J. Gmitter, R. D. Meade, A. M. Rappe, K. D. Brommer, and J. D. Joannopoulos, Phys. Rev. Lett. **67**, 3380 (1991).
[21]D. Pradhan, I. I. Tarhan, and G. H. Watson, Phys. Rev. B **54**, 13721 (1996).
[22]M. A. Kaliteevski, J. Manzanares-Martínez, D. Cassagne, and J. P. Albert, Phys. Rev. B **66**, 113101 (2002).
[23]Described in any crystallography book, see C. Giacovazzo, H. L. Monaco, D. Viterbo, G. Gilli, M. Catti, *Fundamentals of Crystallography* (International Union of Crystallography/Oxford University Press, London, 1992).
[24]J. M. Cowley, *Electron Difracction Techniques*, (Oxford University Press, London, 1992), Vol. 1.
[25]A. Rugge and S. H. Tolbert, Langmuir **18**, 7057 (2002).
[26]Notice that the size difference is within the polydispersity of the two components.
[27]M. Born and E. Wolf, *Principles of Optics* (Cambridge University Press, Cambridge, UK, 1997).
[28]C. Teodosiou, *Elastic Models of Crystal Defects* (Springer, Berlin, 1982).
[29]M. Härting, H. Yaman, R. Bucher, and D. T. Britton, Adv. Eng. Mater. **4**, 592 (2002).
[30]T. Ohashi, J. Phys. IV **Pr9**, 279 (1999).
[31]A. A. Asatryan, P. A. Robinson, L. C. Botten, R. C. McPhedran, N. A. Nicorovici, and C. M. de Sterke, Phys. Rev. E **62**, 5711 (2000).
[32]W. Stöber, A. Fink, and J. J. Bohn, J. Colloid Interface Sci. **26**, 62 (1968).